Measurement of Transverse and Axial Apparent Dispersion Coefficients in Packed Beds

Ulrich Tallarek, Klaus Albert, and Ernst Bayer
Institut für Organische Chemie, University of Tübingen, D-72076 Tübingen, Germany

Georges Guiochon
Dept. of Chemistry, The University of Tennessee, Knoxville, TN 37996 and Chemical and Analytical Sciences Div., Oak Ridge National Laboratory, Oak Ridge, TN 37831

The axial and transverse apparent dispersion coefficients of three solvents in two packed chromatographic columns were determined by pulsed-field-gradient nuclear-magnetic resonance in a range of mobile phase velocity. The column beds were packed with 5-μm particles of porous C18 silica or 30-μm particles of silica. The solvents used were methanol and acetonitrile (in an 80:20 ACN/water solution) in the former case and acetone in the latter. The coefficients were determined over a range of particle Peclet numbers from less than 0.1 to approximately 10 in the former case and 40 in the latter. The data obtained with short dispersion times were fitted to the correlations suggested by Giddings, Horvath and Lin, Huber, and Knox. These data agreed well only with the Giddings equation.

Introduction

The development of preparative liquid chromatography as a large-scale separation process raises new issues regarding the packing of columns. These issues are not found in the packing of analytical columns nor in the packing of the beds used for conventional adsorption processes. Two implementations of the chromatographic process are now considered for large-scale applications, overloaded elution preparative chromatography (OEPC) on wide-bore columns, and simulated moving bed (SMB) using a train of eight to sixteen identical columns having a lower diameter than the unique column used in OEPC for the same production rate. On the one hand, it is more difficult to pack homogeneous columns of large diameter than conventional analytical columns. The specifications for bed homogeneity become more severe when the diameter increases. Fluctuations of the packing density on a scale of the same order as the column diameter cause considerable perturbations in the band profile, due to differential migration (Yun and Guiochon, 1994). This reduces production rate and/or yield. On the other hand, proper operation of SMB requires that the different columns used have nearly identical properties. Otherwise, the production rate may be reduced or instabilities may develop. When the packing densities of the columns are different, so are their permeabilities, retention factors, and efficiencies. If these parameters fluctuate too widely, the process may even become unstable. We must learn to pack columns that have packing densities much closer than achieved with current standards. Significant improvements in the performance of chromatographic processes (Guiochon et al., 1994) and possibly of other adsorption processes would become possible if major progress were made in this area.

Numerous studies on procedures for the packing of analytical columns were carried out in the 1970s (Poole and Poole, 1993). The conventional procedure of slurry packing was developed. With this method, the consolidation of the bed is achieved under the viscous stress caused by a high-velocity solvent stream. Although the efficiency of the columns obtained is usually very good, this method suffers from several important drawbacks. The packing density of the columns is poorly reproducible. The packed bed is not always stable; in many cases, it collapses after a certain period. Finally, the procedure cannot be used for wide-bore columns, which cannot stand the high pressure required. The influence of the parameters of slurry packing on the column efficiency has been abundantly discussed (Poole and Poole, 1993). However, these investigations were entirely empirical and the conclusions of many of them appear to be somewhat contradictory.

Alternative procedures for large-scale columns involve the use of mechanical stress to consolidate the bed. Most common stresses employed are axial (Godbille and Devaux, 1976) and radial (Little et al., 1976) compression. The importance of the compressibility of the packing materials under such mechanical stress has been recognized only recently. Guiochon and Sarker (1995) and Sarker et al. (1996) showed that the packing density of axial compression columns depends to a large extent on the stress applied to the packing. The packing density under axial compression at an applied stress of 100 kg/cm^2 is 25 to 30% higher than the density of the material in its original container (Guiochon and Sarker, 1995). The distribution of mechanical stress inside a bed of pulverulent material cannot be homogeneous (Train, 1957). Hence, the distribution of packing density is not homogeneous either. The packing density of analytical columns prepared by slurry packing is less than the density achieved in axial compression columns (Stanley et al., 1996) and it is less reproducible. The difference between the packing densities of columns prepared in a single batch is usually large enough to prevent accurate predictions of the band profiles on a column from the equilibrium isotherms measured on a different column (Guan and Guiochon, 1995). Such calculations can be done only if the weight of packing in the columns is known.

To summarize, packing materials are compressible; the stress applied to the packing material inside the column, during its packing, is not homogeneous; the column-to-column reproducibility of the packing density is poor. The packing density inside a given column is not homogeneous. The local column efficiency or height of an equivalent theoretical plate (HETP), the local retention factor, the local parameters of the isotherm, and the local permeability depend to some extent on the location. The bands become warped during their migration. As a consequence, the performance of the column decreases with increasing extent of the fluctuations of the local packing density. Fundamental investigations of the dynamics of column packing and of the characteristics of the beds obtained is necessary to improve our ability to pack efficient, reproducible columns for preparative chromatography.

There are a number of reports in the literature demonstrating that the mobile phase velocity and the local HETP are not constant across the column (Knox et al., 1976; Eon, 1978; Baur et al., 1988; Baur and Wightman, 1989; Farkas et al., 1994, 1996). All these authors used ratios of column-to-particle diameter in excess of several hundreds. Knox et al. (1976) and Eon (1978) used a dry-packing procedure (Poole and Poole, 1993) and found the velocity and the HETP to be higher close to the wall than in the center of the column. The other authors used a slurry-packing method and found the velocity to be about 5% lower along the column wall than in its center, while the HETP was several times higher along the wall than in the center. These results confirm those derived from investigation of packing behavior discussed previously. Clearly, a method of investigation of the local properties of the packed bed in a chromatographic column is necessary.

There is a huge amount of literature on hydrodynamic dispersion that cannot be reviewed comprehensively in this work. However, besides the more specialized literature discussed, articles by Ebach and White (1958), Gunn (1968), Gunn et al. (1969), and Hiby (1962) should be acknowledged. These authors have derived correlations between the axial and radial Peclet numbers and the Reynolds number. As we show later in this work, the range of Reynolds number within which liquid chromatography separations are carried out is very low, of the order of 1×10^{-3}. The experimental data on which most correlations have been studied were collected at values of the Reynolds number that are much higher than that, always above 0.1 (Ebach and White, 1958; Gunn, 1968, 1969; Hiby, 1962). Thus, the previous work cannot be used in this case.

Nuclear magnetic resonance (NMR) imaging (Callaghan, 1991) and the related method of pulsed-field-gradient (PFG) NMR (Callaghan, 1984) are now well-established methods, particularly in medicine (Cho et al., 1993; Wehrli et al., 1988), but also in material sciences (Stilbs, 1987; Kärger et al., 1988; Komoroski, 1993). Following the pioneering work of Stejskal and Tanner (Stejskal, 1965; Stejskal and Tanner, 1965; Tanner and Stejskal, 1968; Tanner, 1970), PFGNMR can be used for measuring diffusion coefficients in systems ranging from unrestricted bulk diffusion in liquids (Callaghan et al., 1980) to the much slower motion of, for example, sorbed molecules in zeolites (Kärger and Ruthven, 1992) or restricted diffusion in porous media (Gibbs et al., 1992). These methods can also be implemented for direct investigations of the three-dimensional (3-D) profile of bands migrating along a chromatographic column and *in situ* measurement of the apparent dispersion coefficient in any direction of a packed bed. Results obtained by NMR imaging have demonstrated the warping of chromatographic bands (Tallarek et al., 1995). On the other hand, preliminary data (Baumeister et al., 1995) have shown the local values of the apparent axial and transverse dispersion coefficients to correspond to relatively low values of the local plate height, with a minimum of the relative axial plate height of the order of 1.3, or nearly half the value typically obtained with a well-packed column. The advantage of this method of measurement is that it allows the acquisition of data inside the column, without requiring any injection. The mobile phase itself is used as the probe. This eliminates the contributions of the sources of extra-column band broadening and the influence of the retention. Furthermore, because the apparent dispersion coefficients are measured for low values of the dispersion time, the results are independent of large-scale fluctuations of the local velocity. In this article, we discuss the velocity dependence of the apparent axial and transverse dispersion coefficients and compare several models that have been proposed to account for this phenomenon.

Theory

We characterize the column efficiency using the definition given by Giddings (1965) of the height equivalent to a theoretical plate as the slope of the dependence of the band variance on its migration distance. As a result, we consider the axial and transverse reduced HETP

$$h_a = \frac{H_a}{d_p} = \frac{1}{d_p}\frac{\partial \sigma_a^2}{\partial z}$$

$$h_t = \frac{H_t}{d_p} = \frac{1}{d_p}\frac{\partial \sigma_t^2}{\partial z}, \qquad (1)$$

where H_a and H_t are the axial and transverse HETPs, h_a and h_t the corresponding reduced HETPs.

The axial and transverse dispersion coefficients derived from measurements using the setup and pulse sequences shown in Figure 1 are values of these coefficients averaged over the entire section of the column inside the RF coil, that is, 2.5 to 3 cm long. Thus, we consider here the corresponding axial and transverse HETPs derived by application of the conventional relationships

$$D_{ap,a} = \frac{H_a u}{2} = \frac{h_a \nu D_m}{2}$$

$$D_{ap,t} = \frac{H_t u}{2} = \frac{h_t \nu D_m}{2}, \qquad (2)$$

where $D_{ap,a}$ and $D_{ap,t}$ are the apparent axial and transverse dispersion coefficients, respectively, D_m is the molecular diffusivity, u is the cross-section average mobile phase velocity, and $\nu = ud_p/D_m$ is the reduced velocity or particle Peclet number. The column axis being taken as the axis Oz, a transverse dispersion coefficient can be measured in any direction in the plane (x, y). Because the results of NMR measurements (see later, first paragraph of Results and Discussion section) have shown that the transverse dispersion coefficient does not vary significantly with the direction in which it is measured, we assume that the column has cylindrical symmetry.

Several equations have been proposed to account for the apparent dispersion of bands migrating along a chromatographic column. They are reviewed below.

Simple Giddings equation

Axial dispersion is due to a combination of molecular and eddy diffusion. Molecular diffusion is caused by concentra-

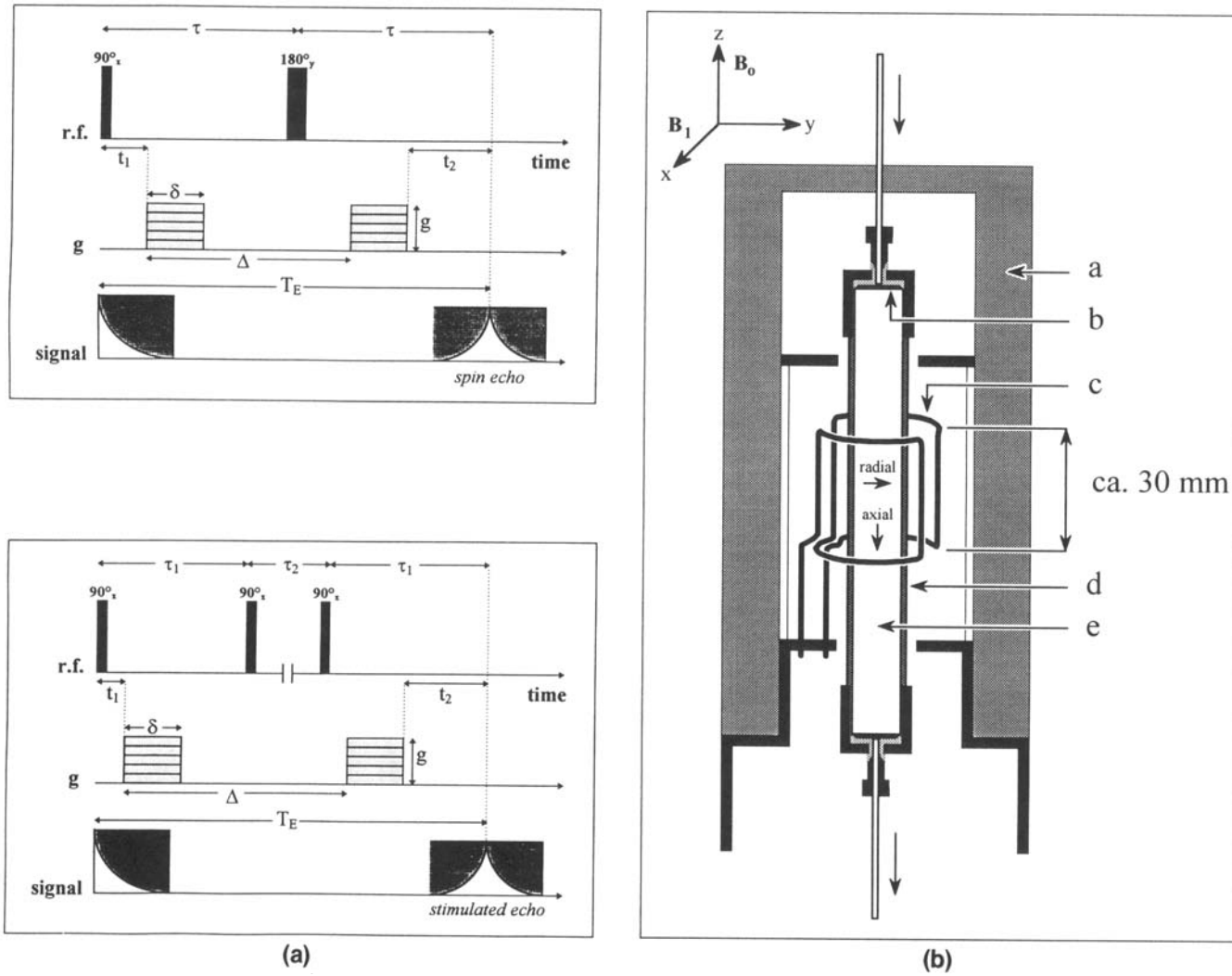

Figure 1. The instrument.

(a) The pulse–echo sequences. Pulsed-field-gradient spin echo (PFGSE, upper part) and pulsed-field-gradient-stimulated echo (PFGSTE, lower part) sequences with gradient amplitude, g, gradient pulse duration, δ, and interpulse spacing, Δ. In the spin echo version, τ is the time between the $90°_x$ and $180°_y$ r.f. pulses and corresponds to half the spin echo formation time, T_E. In the stimulated echo version, the echo time is given by $T_E = 2\tau_1 + \tau_2$.

(b) The liquid-chromatograph–NMR spectrometer setup used for PFGNMR dispersion measurements in chromatographic columns. a: microimaging gradient system; b, PEEK frit; c, 15-mm r.f. insert; d, PEEK column (4.4-mm ID); e, porous packing in the column.

tion gradients that exist necessarily when a zone of finite length migrates along a column. It follows Fick's law. However, since diffusion cannot proceed along a straight line in a packed bed, the apparent axial diffusion coefficient is lower than the molecular diffusivity, a phenomenon accounted for by the introduction of the tortuosity coefficient in the HETP equations (see later) (Giddings, 1965). Eddy diffusion results from the inequalities of the local values of the linear velocity in the different channels available to the stream. It should be noted that liquid chromatography is carried out under experimental conditions such that the Reynolds number is extremely low. The Reynolds number can be rewritten as

$$Re = \frac{ud_p\rho}{\eta} = \nu\frac{D_m\rho}{\eta}. \tag{3}$$

Typical values of ρ and η for the mobile phase are 0.8 g/mL and 0.01 P, respectively, with a range of values not exceeding 20 and 50%, respectively, in actual practice. The flow rate is usually selected so that the reduced velocity is between 5 and 15. With molecular diffusivity ranging between 1×10^{-5} and 1×10^{-6} cm^2/s for most components separated in liquid chromatography, the Reynolds number is of the order of 1×10^{-3} in most cases, indicative of a creeping laminar flow, with negligible turbulence (Bird et al., 1960). (N.B. Obviously, the Reynolds number is independent of molecular diffusivity; this parameter is used here only as an intermediate in the calculation of typical values of the Reynolds number for typical chromatographic conditions.)

Giddings (1965) has shown that eddy diffusion depends on the mobile phase velocity, in contrast with what a simple model of this effect would predict. A molecule that is in a fast stream path takes a step forward with respect to the zone. This step can end either because the velocity of the stream path decreases (because of the complexity of the channel network, velocities at different positions along a given stream path are unrelated) or because the molecule jumps by diffusion from one stream path to another. Thus, diffusion relaxes the radial concentration gradient that tends to be built up by the inequalities in the local flow velocity. Applying the random-walk relationship to a model of eddy diffusion incorporating this coupling between transverse diffusion and spacial fluctuations of the velocity, Giddings (1965) developed a plate-height equation, by analogy to conductors in parallel. This equation is given by

$$h = \frac{2\gamma}{\nu} + \frac{2\lambda}{1+\omega\nu^{-x}} + C\nu, \tag{4}$$

where γ is the tortuosity coefficient, λ and ω are geometrical parameters and functions of the retention factor, and x is a constant equal to 1. The random-walk relationship used is tantamount to assuming a linear dependence of the convective mass-transfer rate on the velocity. This is a simplification that appears to be valid in the velocity range used in chromatography but may falter at higher velocities. Finally, we note that the simple Giddings equation lumps together the transverse convective/diffusive relaxation of the effect of the heterogeneity of the axial velocity with film mass transport. The third term in Eq. 4 is proportional to the reduced velocity; hence it can account only for mass-transfer processes taking place inside the particles.

Based on Eq. 4, it is possible to write the following equation for the transverse reduced plate height

$$h_t = \frac{2\gamma}{\nu} + D, \tag{5}$$

where D is a coefficient accounting for the contribution of eddy diffusion to transverse dispersion. This last contribution has been explained in the literature by the phenomenon of "stream splitting" (Saffman, 1959, 1960; Horne et al., 1966; Littlewood, 1966), as explained later. The first term in the righthand side (RHS) of Eq. 5 represents the diffusion contribution to the transverse reduced plate height.

Comprehensive Giddings equation

Eddy diffusion results from the inequalities of the local velocity. Such inequalities arise at different scales inside the column. Although there is a continuous distribution of these scales, Giddings has divided them into four different levels: (1) the transchannel contribution to band spreading arises from the radial distribution of velocities inside each individual channel; (2) the short-range interchannel contribution is due to the existence of small groups of tightly packed particles between which more loosely packed regions are found; (3) the fluctuations of local packing density causes this pattern of tightly packed groups of particles interspersed by loosely packed regions to be erratic, which results in the long-range interchannel contribution; and (4) the existence of systematic variations of the mobile phase velocity between different regions of the column (i.e., in the center and the outer regions) is responsible for the transcolumn contribution. Each of these effects introduces a term similar to the one derived from the coupled theory and given in Eq. 4. The comprehensive equation that accounts for all the possible contributions related to eddy diffusion becomes

$$h = \frac{2\gamma}{\nu} + \Sigma_i \frac{2\lambda_i}{1+\omega_i\nu^{-1}} + C\nu, \tag{6}$$

where the coefficients λ_i and ω_i correspond to the velocity inequality of type i among the four listed earlier. This equation is complex and difficult to use. The determination of the numerical values of these coefficients would be a most arduous experimental task. It has never been undertaken, as far as we know. The values estimated by Giddings (1965) on a theoretical basis for the transchannel, short-range interchannel, long-range interchannel, and transcolumn effects are $2\lambda = 0.5$, 0.5, 0.1, and 0.04 m^2 (m, ratio of column to particle diameters) and $\omega = 100$, 2.0, 0.1, and 40, respectively. Efforts to reduce Eq. 6 to practice have led to the Knox equation (see later).

Huber equation

Using a correlation derived through a dimensional analysis of the data collected by Hiby (1962), Huber (1973) calculated the dispersion term arising from the nonuniformities of the flow and derived the plate-height equation given by Eq. 4

with $x = 0.5$. Note that the constants ω and C have different physical meaning and different dependence on the packing characteristics in the Giddings, the Huber, and the Horvàth–Lin equations.

Horvàth and Lin equation

Horvàth and Lin (1976) considered the stagnant film of mobile phase surrounding each particle in the bed and assumed that axial dispersion takes place only in the fluid outside the stagnant film. The thickness of this film, δ, decreases with increasing mobile phase velocity. Pfeffer and Happel (1964) have shown that the Sherwood number, $Sh = k_f d_p/D_m$, increases in proportion to the power 1/3 of the reduced velocity. Horvàth and Lin (1976) have assumed that δ is equal to the thickness of the Nernst diffusion layer, D_m/k_f, with k_f rate constant of mass transfer. Thus, from this dependence of the rate of mass transfer on the reduced velocity, they obtained

$$\delta = \frac{d_p}{\omega \nu^{0.33}}. \tag{7}$$

Using this value of the thickness of the stagnant film, they derived a plate-height equation that is given by Eq. 4 with $x = 0.33$.

Horvàth and Lin (1976, 1978) have shown that their model is consistent with their experimental results, although this does not constitute a proof of its validity, given the complexity of the relationship involved.

Comparison of the three equations

The equation derived by Huber (1973) is not based on a physical model but on an empirical correlation, the accuracy of which has been questioned (Deelder, 1970). Horvàth and Lin (1976) did not attempt to calculate a coupling effect between molecular and eddy diffusion. They only assumed that the volume of the extraparticle space in which eddy diffusion takes place is reduced by a film of stagnant mobile phase velocity. However, it seems that the thickness of this film is constant in the range of reduced velocities within which liquid chromatography is usually carried out and within which eddy diffusion is encountered and is found to vary with the flow velocity. Arnold et al. (1985) explained that the relationship derived by Pfeffer and Happel (1964) between the Sherwood number and the reduced velocity is valid only at large velocities, for $\nu > 50$. At lower values of the velocity, the Sherwood number would approach a constant limit and so also would the mass-transfer coefficient and the thickness of the stagnant boundary layer (Pfeffer and Happel, 1964). Under such conditions, the Horvàth–Lin equation would reduce, like the Giddings equation, the Huber equation, and Eq. 4 to the Van Deemter (1956) equation (Eq. 9), with $A = 2\lambda$. However, Nelson and Galloway (1975) have shown that, although the Sherwood number is constant at lower values of the velocity for a single particle, this result is not true for densely packed particle beds. In this case, the Sherwood number becomes proportional to the Reynolds number at low flow rates. If this dependence is substituted in the thickness of the Nernst layer (Eq. 7), the Giddings equation (Eq. 4 with $x = 1$) is obtained instead of the Horvàth and Lin equation (Eq. 4 with $x = 0.33$).

Early experimental results by Giddings and Robison (1962) have shown that the conventional expression of the eddy diffusion term used in Eq. 9 and other related plate-height equations is not valid. They studied eddy diffusion in gas chromatography using a 12 m long, 1/4 in. (6.4 mm) OD (presumably, 4.6 mm ID) column, packed with 1.17 ± 0.1-mm-dia. glass beads, nitrogen as the carrier gas, and carbon dioxide and *p*-xylene vapor as the sample (diffusivity, 0.073 cm/s^2; Giddings, 1965). Measurements were carried out very carefully in a range of reduced velocity extending from 0.2 to 2.3. In this range, a plot of h vs. $1/\nu$ is linear and has a very small intercept (and a slope corresponding to $\gamma = 0.735$). The value of ω was very large, probably well above 10, effectively rendering the eddy diffusion term negligible. This is expected as the column having a ratio d_c/d_p of 4 can hardly accommodate more than one channel. It is remarkable that the value of h for the five data points at reduced velocities larger than 1.0 are all below 1.0, with one value of h reported at 0.5. This work, however, did not attempt any investigation of the $h(\nu)$ relationship at higher reduced velocities, which would have been experimentally most difficult at the time. Sternberg and Poulson (1964) demonstrated that the minimum value of h is below 1 for columns packed with glass beads larger than 0.1 times the column diameter. Halasz and Heine (1962) also obtained values of h lower than 1 with drawn-glass packed capillary columns. Other works from Giddings on the efficiency of gas chromatographic columns reported a few values of h below 1.0 (e.g., Giddings, 1963).

A careful experimental study of this problem has been made by Magnico and Martin (1990). These authors packed a 16.6×2.4 cm column with 200–220 μm solid glass beads, taking great care to achieve an homogeneous bed by ensuring radial homogeneity of the flux of new beads carried by a water stream to the top of the bed. They measured the profiles of breakthrough curves of concentration steps of solutions of nonretained salts. The profiles were found to be well accounted for by an error function (erf), as expected under linear conditions (which should prevail since there is no retention). The HETP derived from the variance of these erf functions was measured at different flow rates corresponding to reduced velocities between 0.5 and 300. The data are in excellent agreement with the prediction of the Giddings equation (Eq. 4 with $x = 1$). They falsify the other two equations (Eq. 4 with $x = 0.5$ or 0.33). It is useful to note that the minimum value found for the HETP was 1.0, achieved for a reduced velocity of about 3.

The excellent agreement reported by Magnico and Martin (1990) between the Giddings equation and their experimental data demonstrates that either one of the four different levels of flow nonuniformities distinguished by Giddings is affecting the column efficiency in their experiment or that, if several of them are involved, they have similar values of ω. By parameter identification, they derived from their data values of $2\lambda = 1.06$ and $\omega = 10.3$. The values estimated by Giddings (1965) on a theoretical basis for the transchannel, short-range interchannel, and long-range interchannel effects are $2\lambda = 0.5$, 0.5, and 0.1 and $\omega = 100$, 2.0, and 0.1, respectively. The authors conclude that, since transchannel effects are always present and since it is impossible to avoid any short-range interchan-

nel effects, their data must reflect some combinations of these two effects.

Knox equation

Kennedy and Knox (1972) have shown that a simple additive contribution, $a\ \nu^{1/3}$, to the plate-height equation can account for the combination of the effects of the four different levels of flow nonuniformities distinguished by Giddings (1965), transchannel, short-range interchannel, long-range interchannel, and transcolumn effects. The replacement by this term of the complex sum of four terms in Eq. 6 causes a considerable simplification. The resulting plate-height equation is known as the Knox equation

$$h = \frac{b}{\nu} + a\nu^n + c\nu, \tag{8}$$

where a, b, c, and n are numerical coefficients, functions of the nature of the packing material used, of the compound studied, and of the homogeneity of the column bed. The first term in the RHS of Eq. 8 accounts for axial diffusion, the second for a combination of axial dispersion and eddy diffusion, the last one for the mass-transfer kinetics in the linear case. The exponent n is between 0.2 and 0.35. It is often taken as equal to 0.33 in the chromatographic literature (Knox, 1977), although it was set at 0.2 in some early work (Eon, 1978). Equation 8 is an empirical correlation that is in agreement with most experimental results (Horne et al., 1966; Knox and Saleem, 1969; Eon, 1978; Unger et al., 1978), provided they are acquired in a sufficiently wide range of flow rates. Thus it is possible to separate the contributions of the last two terms in the RHS of Eq. 8. The minimum value of h is achieved for values of ν around 3. It seems that data have to be acquired in a velocity range from 0.5 to 50 to provide a reasonable precision of the estimates of the three coefficients obtained by identification.

However, in a number of cases (e.g., Katz et al., 1983), mainly because experimental data are acquired in too narrow a range of reduced velocities, the data fit at least as well to the Van Deemter (1956) equation

$$h = a + \frac{b}{\nu} + c\nu. \tag{9}$$

This latter model does not account for the flow-rate dependence of the eddy diffusion term that is weak but becomes noticeable when measurements are carried out in a range of mobile phase velocities exceeding an order of magnitude.

The Knox equation is much simpler and practical than the complete plate-height equation by Giddings (Eq. 6) and about as correct for columns of moderate or good efficiency. The determination of all the eight parameters of Eq. 6 from experimental data is practically impossible. However, the Knox equation is not expected to work as well as the Giddings equation when the column efficiency is high, as in the case of the study made by Magnico and Martin (1990).

Transverse dispersion and stream splitting

When a zone migrates along a chromatographic column, it is dispersed both axially and radially by a combination of diffusive and convective processes. When a streamlet hits a particle, it splits into several, unequal streamlets that flow around the hit particle, between it and its different neighbors, and merge with other different streamlets of similar origin. Transverse diffusion in the new streamlets and a cascade succession of similar events at each particle encountered promote transverse dispersion. Because the average width of streamlets in a packed bed is much smaller than one particle diameter, typically of the order of $0.1 d_p$ or less, local transverse homogenization of the mobile phase composition takes place quickly. It is much slower at the scale of the column diameter, however.

Saffman (1959, 1960) investigated the problem rigorously, using a random-walk model. He assumed that there is no adsorption, the medium is isotropic, and the mean pressure gradient is constant. The column is supposed to consist of a network of randomly oriented capillary tubes. Two problems were successively solved. First, molecular diffusion was neglected compared to convective dispersion (Saffman, 1959). Later, a more sophisticated model allowed the derivation of a solution in the case in which transfer by molecular diffusion is significant (Saffman, 1960). In chromatography, however, separations are carried out under conditions such that the reduced velocity always exceeds 2 and is often between 5 and 10. So, we can consider only the former, simpler solution that gives for the transverse dispersion coefficient

$$D_{ap,r} = \gamma D_m + \frac{3u}{16 d_p}. \tag{10}$$

Hence

$$h_r = \frac{2\gamma}{\nu} + 0.375. \tag{11}$$

Horne et al. (1966) applied the classic random-walk model of chromatography developed by Giddings (1965). They assumed that the particles are spherical and that, when a streamlet hits a sphere, it divides equally around it. This causes the average molecule to undergo a transverse step of average length d_p/π. The radial variance contribution, according to the random-walk model is nl^2, with n = number of steps, and l = average length of a step. Assuming that one lateral step is taken for every distance $a\ d_p$ moved axially (with a = a number between 0 and 1), they derived a variance contribution equal to $Ld_p/(a\ \pi^2)$. The corresponding contribution of stream splitting to the reduced HETP is

$$h_c = D = \frac{1}{a\pi^2}. \tag{12}$$

In a dense packing such as the bed of a chromatographic column, it is reasonable to expect that a is between 0.5 and 1, giving a value of D between 0.1 and 0.2. Within this range, D could be a function of the particle shape and of the packing density.

There are few determinations of D in the chromatographic literature. Using systematic determinations of the elution profiles in a number of points scattered over the cross-sec-

tion area of the exit frit of a column, Knox et al. (1976) derived for D a value of 0.060. The experimental data were acquired for values of ν between 16 and 250, with a 11.7 mm ID column packed with 64-μm glass beads. Using a similar method, Eon (1978) derived a value of D equal to 0.075, the measurements being made for values of ν between 0.6 and 1000, using a 17-mm-ID column packed with 76-μm glass beads. Using on-column NMR measurements of the transverse dispersion coefficients on a 26-mm-ID column packed by gravity sedimentation with 15-μm silica particles, Baumeister found a value of D equal to 0.201. Given the packing procedure, a markedly lower packing density was achieved in this experiment than in those using a more classic packing method, even dry-packing as used by Knox et al. (1976) and Eon (1978).

Determination of diffusion and apparent dispersion coefficients by NMR

In a homogeneous magnetic field, the spin of a given nucleus precesses around the direction of this field at the Larmor frequency, ω_0, which is related to the field intensity, B_0, by

$$\omega_0 = \gamma B_0, \tag{13}$$

where γ is the gyromagnetic ratio of the nucleus being considered (Abragam, 1961; Slichter, 1963). In the case of protons ($\gamma = 2.675 \times 10^8$ rad$\cdot$s$^{-1}\cdot$T^{-1}), in a large superconductive magnet where $B_0 = 9.4$ T, this frequency is $\nu_0 = \omega_0/2\pi = 400$ MHz. Thus, nuclear magnetic resonance provides a molecular label via the characteristic Larmor frequencies of the component nuclei, most commonly the protons. In a magnetic field gradient, each proton is provided with an address corresponding to the exact field at the time of excitation. In practice, the spatial dependence of the label is given by the imposition over the sample space of a well-defined pulsed-magnetic-field gradient, characterized by its strength g, its duration δ, and its direction. This pulse causes the proton spins to precess at different frequencies, according to their locations r along the direction of the applied gradient (Callaghan, 1991). Hence, we can define a local Larmor frequency as

$$\omega(r) = \gamma B_o + \gamma g r. \tag{14}$$

Very sensitive precessional phase displacements may be detected through the degree of phase refocusing in an NMR spin echo. Hahn (1950) was the first to suggest that these echo signals might be used to measure molecular translational motions and to propose the spin echo experiment. The pulsed-field-gradient nuclear magnetic resonance (PFGNMR) spin echo method in its simplest form consists of a two-r.f.-pulse Hahn echo experiment with identical magnetic-field-gradient pulses of magnitude g and duration δ. These two pulses are separated by a time Δ. They are applied respectively during the dephasing and rephasing parts of the echo cycle (see Figure 1a, upper part). After irradiation of the proton spins by a nonselective 90° pulse, the first gradient pulse produces a rapid precessional phase shift depending on the position of each nucleus in the sample. Between the two gradient pulses the molecules containing the spatially labeled nuclei change position, for example, because of diffusion, dispersion, or convection. During this period, the nonselective 180°C r.f. pulse has inverted all prior phase shifts. Thus, the second gradient pulse, at time $t_1 + \Delta$, has the effect of producing phase compensation (or refocusing). To the extent that molecular motion has occurred, the refocusing is incomplete and the consequent attenuation of the intensity of the spin echo (located at time $t = 2\tau = t_1 + t_2 + \Delta + \delta$) gives a measure of the ensemble average of the nuclear translations. The larger the gradient strength used to label the spins, the stronger this echo attenuation. The two gradient pulses record the initial and subsequent positions of the nuclei over the well-defined time scale Δ, respectively. A series of spin echo spectra is recorded while incrementing the gradient strength from one experiment to the next. The echo intensities display a characteristic Gaussian distribution for unrestricted isotropic diffusion. Usually the intensities are analyzed in terms of the Stejskal–Tanner equation (Stejskal and Tanner, 1965; Callaghan, 1991)

$$\frac{M(\boldsymbol{k}, \Delta)}{M(0, \Delta)} = e^{-k^2 D(\Delta - \delta/3)}, \tag{15}$$

where $\boldsymbol{k} = \gamma\delta\boldsymbol{g}$, $\boldsymbol{g}$ is the gradient strength and direction, δ is the pulse duration, γ is the gyromagnetic ratio, Δ is the pulse period, and $\Delta_r = \Delta - \delta/3$ is the reduced or effective diffusion time. $M(0, \Delta)$ is the echo intensity obtained in the absence of any pulsed field gradient ($g = 0$), so $\boldsymbol{M}(\boldsymbol{k}, \Delta)/M(0, \Delta)$ is the normalized amplitude. In practice, the intensities are plotted as $\log [\boldsymbol{M}(\boldsymbol{k}, \Delta)/M(0, \Delta)]$ vs. g^2 or k^2 and the diffusion coefficient is derived from the slope of the corresponding plot.

Incorporating the effect of a convective displacement caused by the flow velocity and superimposed on the dispersion is straightforward. The combined effect of diffusion or dispersion and flow on the echo signal is a phase shift due to the flow and an attenuation due to the diffusion, the global effect being given by

$$\frac{M(\boldsymbol{k}, \Delta)}{M(0, \Delta)} = e^{i\boldsymbol{k}\boldsymbol{v}\Delta - k^2 D(\Delta - \delta/3)}, \tag{16}$$

where $\boldsymbol{v}$ is the mean flow velocity (Callaghan, 1991). It is important to note that an attenuation of the signal intensity is caused only by diffusion. Therefore, by phase correcting successive spectra or recording them in the magnitude mode instead of the absorption mode, diffusion effects can be well resolved from flow effects, the latter assigning a characteristics phase shift to the signal because of their coherent nature.

This method allows the determination of diffusion or dispersion coefficients in the presence of flow. In some circumstances, however, short transverse nuclear relaxation times T_2 limit the spin echo signal-to-noise (S/N) ratio. Moreover, irreversible decay due to spin-spin (transverse) relaxation limits the time Δ over which PFGNMR measurements are possible. These problems associated with the short T_2 can be circumvented sometimes, especially where the spin-lattice (longitudinal) relaxation time, T_1, greatly exceeds T_2. In this case, the stimulated echo method can prove useful (Tanner, 1970; Stilbs, 1987; Kärger et al., 1988) (see Figure 1a, lower

part). In this method, the 180° r.f. pulse is divided into two successive 90° r.f. pulses. The stimulated echo center is located at $t = 2\tau_1 + \tau_2$. During time τ_2 (the major part of the diffusion time, Δ), the spatially labeled spins are subject to longitudinal instead of transverse relaxation, because the second 90° pulse, after τ_1, rotates the magnetization into the longitudinal direction, that is parallel to the direction of the main magnetic field.

Experimental Studies

Chromatography

No samples were injected into the chromatographic column to perform the NMR experiments. Instead, pure solvents or solvent mixtures were pumped through the chromatographic column under study. Thus, no injection valves and no detectors were needed. The pump must maintain a constant mobile phase flow rate in the range investigated (0.01–4.6 mL/min). Altogether, this made the experiment design most simple.

No metal can be introduced inside or placed close to the magnet, however, as it would cause too strong perturbations of the magnetic field and would interfere with the signal. For this reason, it was not possible to use an axially or radially compressed column in these experiments. The design of a nonmetallic skid is still under active consideration. Accordingly, the 4.4-mm-ID, 10-cm-long columns were made of PEEK (poly (aryl ether ether ketone)), a high tensile plastic material, were closed with PEEK frits (Upchurch Scientific, Oak Harbor, WA), and were connected to the pump and the waste collection by narrow-bore PEEK tubings. PEEK unions, *fingertights*, and end column fittings were manufactured out of PEEK rods in the workshop of the University of Tübingen. They were modeled on conventional high-performance liquid chromatography (HPLC) hardware. A Bischoff micropump head (Bischoff, Leonberg, Germany) was adapted to the Bischoff pump for the low flow-rate measurements (0.01–0.6 mL/min). The pump being located several meters from the magnet can be of conventional design and materials. A conventional analytical head was used for flow rates up to 4.6 mL/min. The flow rate was derived by measuring the volume of effluent collected during a given time. The pump was placed about 1.5 m away from the magnet. Precolumn filters were used at the pump outlet to keep the column itself free from impurities (e.g., metal particles) originating from the pumping system.

The PEEK columns were packed with one of the two materials used in this study, adapting the slurry-packing method. An approximately 5% slurry of the packing material in degassed isopropanol (which wets well C_{18} silica) is placed in a stainless steel container that is connected at its outlet to the column, at its inlet to a hydropneumatic HPLC pump (Knauer, Berlin, Germany). The slurry is then forced into the column by pumping degassed methanol with the pump into the container and through the column (Poole and Poole, 1993). The inlet pressure is raised to 300 atm, and the packing material is consolidated for 25 to 35 min under the viscous stress caused by the solvent stream.

Two packing materials were used. LiChrosorb RP18 is a chemically bonded C18, porous, irregular silica with an average particle size of 5 μm. The other material was a 30-μm particle, porous, spherical silica from YMC (YMC Europe, Schermbeck, Germany). The PEEK frits used were 0.5 μm for the 5-μm particle material and 0.5 μm for the 30-μm particle material. The solvents used were acetone, acetonitrile, methanol, and water from Merck (Darmstadt, Germany). They were used as received, without further purification, but were degassed prior to their use in the experiments.

The efficiency of the second column (5-μm LiChrosorb C18 particles) was determined following the conventional chromatographic procedure (Poole and Poole, 1993), using a conventional liquid chromatograph assembled with the same Bischoff HPLC pump as used in the NMR experiments, very short connecting tubes, a 10-μL Rheodyne valve (Cotati, CA), a LINEAR UVVIS 200 spectrophotometric detector (LINEAR Instruments, Reno, NV) operating on the bulk eluent, and a Kipp and Zonen (Schönberg, Germany) BD8 chart recorder. The values of the HETP were measured for toluene, which is very slightly retained, in 80:20 acetonitrile as the mobile phase, at flow rates between 0.1 and 4.5 mL/min.

Nuclear magnetic resonance

NMR experiments were performed at 19 ± 0.5°C on a Bruker (Karlsruhe, Germany) MSL 200 spectrometer equipped with an Oxford 4.7-T, 8.9-cm-bore superconducting magnet. A Bruker imaging probe with a 15-mm-ID "saddle" r.f. insert was used, and the gradient coils were driven by a stereo power amplifier (Model 2200) from NAD Electronics Inc. (Boston, MA). The magnet has a static field strength of 4.7 T, yielding a proton resonant frequency of 200.13 MHz. Data acquisition was controlled by an Aspect 3000 computer. The final spectral linewidths of water, methanol and acetonitrile were around 35-40 Hz in the porous packing in the absence of externally applied magnetic field gradients.

The 90° pulse duration was approximately 20 μs. Field-gradient pulses were applied to the sample using a Bruker microimaging gradient system consisting of three mutually orthogonal coil groups that can produce pulse-field gradients in any direction respective to the axis of the main magnetic field. Gradient pulse intensities g were varied between 0.2 and 32 G/cm (1 Gauss = 10^{-4} Tesla), with a duration δ of 3 and 5 ms, respectively. The values selected for the diffusion time, Δ, were between 30 and 80 ms. PFGNMR experiments were generally performed using fixed echo time and duration of the gradient pulses and varying only the gradient intensity by suitable incrementation. The PEEK columns are directly inserted into the imaging probe, using a special home-built sample holder that makes impossible any column movement during the measurements. The entire system is schematized in Figure 1b. Finally, the column axis is parallel to the axis of the main magnetic field.

Procedures

Orienting the pulsed-field gradients either in the direction parallel to the column axis or in any perpendicular direction, it is possible to measure independently the axial and the transverse apparent dispersion coefficients as a function of the mobile-phase flow velocity. These dispersion experiments were performed with either the standard Stejskal–Tanner pulse sequence (spin echo) or the stimulated echo version (PFGSE and PFGSTE, respectively). The latter method is

Table 1. Coefficients of Self-Diffusion*

Solvent	Apparent Transverse-Dispersion Coefficient	Apparent Axial-Dispersion Coefficient	Coefficient of Self-Diffusion (cm^2/s)
Acetone	1.94	2.04	4.08
Acetonitrile (ACN/H_2O, 80:20)	1.85	1.92	2.75
Methanol	1.19	1.25	1.98
Water			1.98

*In 10^{-5} cm^2/s.

advantageous for the systems under study because the proton relaxation times T_1 for the fluids in the porous matrix are much larger than the corresponding relaxation times T_2. As explained earlier, the effects of dispersion and flow velocity on the resonance signal can be well separated and determined. The combined effect of both factors on the echo signal is a phase shift due to the mobile phase flow rate (first term in the exponent) and an attenuation due to dispersion (second term).

The results are plotted as log $[\boldsymbol{M}(\boldsymbol{k}, \Delta)/\boldsymbol{M}(0, \Delta)]$ vs. the squared gradient intensity, g^2 (Eq. 15). A straight line is observed, indicating that background gradients are negligible in our experiments. The coefficient of apparent dispersion is derived from the small-$\boldsymbol{k}$ dependence of the amplitude, $\boldsymbol{M}(\boldsymbol{k}, \Delta)$, as the slope of this plot. To achieve a sufficient signal-to-noise ratio, $\boldsymbol{M}(\boldsymbol{k}, \Delta)$ and $M(0, \Delta)$ were determined as the averages of up to 64 repetitions of the relevant pulse sequence. Usually, the gradient strength is incremented in 16 steps and D_{ap} is determined by a least-squared fit to the corresponding data set.

The coefficients of self-diffusion and diffusion obtained this way for the solvents studied are reported in Table 1. These data were derived from measurements made on the chromatographic columns in the absence of flow and on samples of the pure liquids, respectively. For each data set linear regressions yield a correlation coefficient of at least 0.999. The self-diffusion coefficient of pure water was found to be 1.96×10^{-5} cm^2/s at 19°C. This value agrees very well with the one obtained by extrapolation of Mills data (I.e., 1.98×10^{-5} cm^2/s), a value that is often used as a reference. The values of the self-diffusion coefficients of normal and heavy water between 1 and 45°C obtained by Mills (1973) are considered as very accurate and precise. They were determined using radioactive tracer methods.

The value of the diffusion coefficients measured in the axial direction in the absence of flow are a few percents higher than in the radial direction. It is interesting to note that the same result was observed previously (Baumeister et al., 1995), in a study using a different instrumental setting, in which the column axis was perpendicular to the axis of the main magnetic field, while these axes are superimposed in the experiments reported here. In both cases, however, the axial dispersion coefficient is only 2 to 7% higher than the transverse dispersion coefficients in the absence of flow.

Results and Discussion

As indicated earlier, the values of dispersion coefficients reported here are averaged over the entire column cross section and over a length of 30 mm. Axial dispersion coefficients are measured by sending the pulse of magnetic field gradient

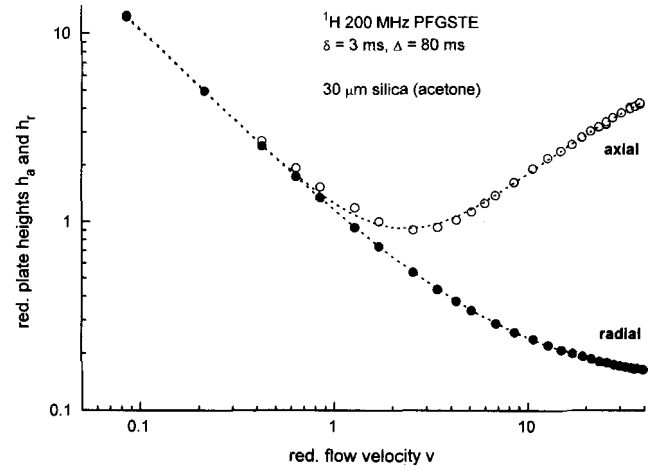

Figure 2. Axial (○) and radial (●) reduced plate height vs. the reduced velocity.

Column packed with 30-μm particles of silica from YMC. Solvent: acetone. Symbols, experimental data; lines, plots of Eqs. 4 (for $x = 1$) and 5.

in the Oz direction (i.e., along the column axis). Transverse coefficients are measured by sending this pulse in any direction of the x, y plane. It has been verified that the gradients in both directions were equally calibrated. The transverse dispersion coefficient was measured in different directions perpendicular to the column axis, by rotating the direction of the pulsed magnetic field gradient. In all cases, it was found that the values obtained were not significantly dependent on the radial direction. Within the experimental errors, the two columns used in this work can be considered as having a cylindrical symmetry.

Figures 2 to 6 show plots of the reduced plate height vs. the reduced velocity under three different sets of experimental conditions. The data obtained on the column packed with 30-μm particles of silica are reported in Figure 2. The data obtained with the column packed with 5-μm particles of silica are reported in Figures 3 (mobile phase, 80:20 solution of

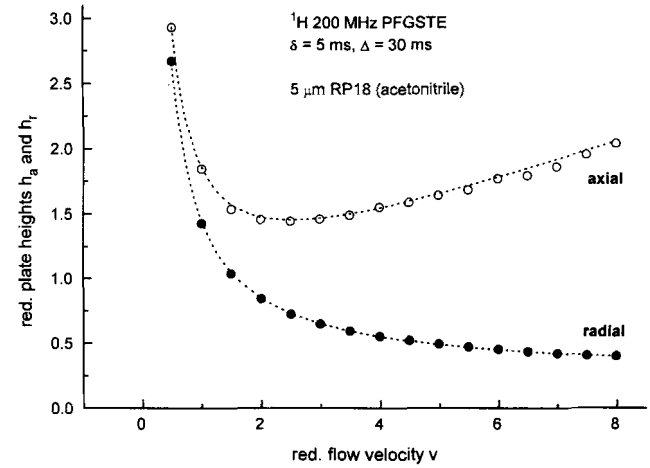

Figure 3. Axial (○) and radial (●) reduced plate height vs. the reduced velocity.

Column packed with 5-μm particles of Lichrosorb RP18. Solvent: methanol. Symbols, experimental data; lines, plots of Eqs. 18.

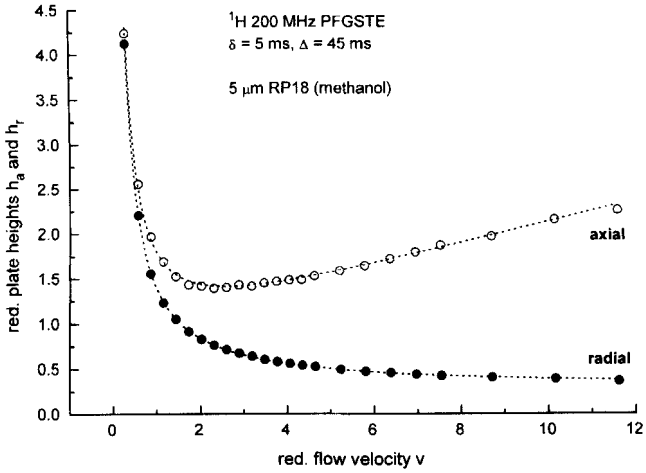

Figure 4. Axial (○) and radial (●) reduced plate height vs. the reduced velocity.

Column packed with 5-μm particles of Lichrosorb RP18. Solvent: methanol. Symbols, experimental data; lines, plots of Eqs. 19.

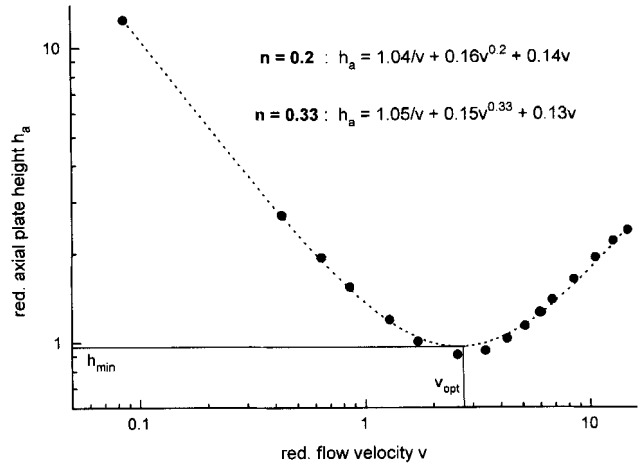

Figure 5. Axial reduced plate height vs. the reduced velocity.

Experimental data (symbols) compared with Eq. 9 (line). Column packed with 30-μm particles of silica from YMC. Solvent: acetone. The contribution of the second term of the RHS is negligible and the two lines are practically overlaid.

acetonitrile and water) and 4 (mobile phase, pure methanol). There is a small scatter of the data points (symbols) around the best curves obtained by fitting these data to Eq. 4 with $x = 1$ in Figure 2, to Eq. 5 or 10 in Figures 3 and 4. It was not possible to measure accurate values of the dispersion coefficients at values of the reduced flow velocity higher than 12 with the 5-μm particle column because the corresponding actual velocity is too large. A fraction of the labeled protons carried downstream by the mobile phase escapes from the volume in which their signal is measured. When this fraction becomes too large, the measurements are no longer accurate.

The nonlinear regressions were done using Eq. 9 for the axial dispersion coefficient and Eq. 5 for the transverse dispersion coefficient. In Eq. 9, we took $n = 0.33$, in compliance with the tradition among chromatographers. As a matter of fact, it was not possible to distinguish between the best curves supplied by a linear regression of the data to Eq. 9 using $n = 0.20$ and $n = 0.33$ (Figure 5). The nonlinear regression gives the following best equations:

—For the data in Figure 2 (30-μm silica particles, acetone):

$$h_a = \frac{1.05}{\nu} + 0.15\nu^{0.33} + 0.13\nu \tag{17a}$$

$$h_r = \frac{1.03}{\nu} + 0.14. \tag{17b}$$

The confidence level of the fit is 0.9997 for the axial reduced HETP, provided the data points beyond $\nu = 15$ are excluded. Otherwise a systematic deviation takes place (see the later discussion). Figure 5 compares a plot of this limited set of experimental data (symbols) and Eq. 17a (dashed line). The systematic deviations taking place around the curve minimum and at high velocities are obvious. The coordinates of the minimum of the $h_a(\nu)$ plot are $h_{min} = 0.91$ and $\nu_{opt} = 2.5$. The confidence level of the fit is 0.999 997 for the transverse reduced HETP, in the whole range of data points. Note that the minimum value of h observed is lower than 1.0, in agreement with data previously reported by Giddings (1963) and Giddings and Robison (1962) (more on this result later).

—For the data in Figure 3 (5-μm silica particles, acetonitrile/water, 80:20):

$$h_a = \frac{1.35}{\nu} + 0.62\nu^{0.33} + 0.12\nu \tag{18a}$$

$$h_r = \frac{1.32}{\nu} + 0.27. \tag{18b}$$

The confidence level of the axial HETP fit is 0.998 (all data points included). The coordinates of the minimum of this plot are $h_{min} = 1.58$ and $\nu_{opt} = 2.4$. The confidence of the fit of the reduced transverse HETP is 0.999 8.

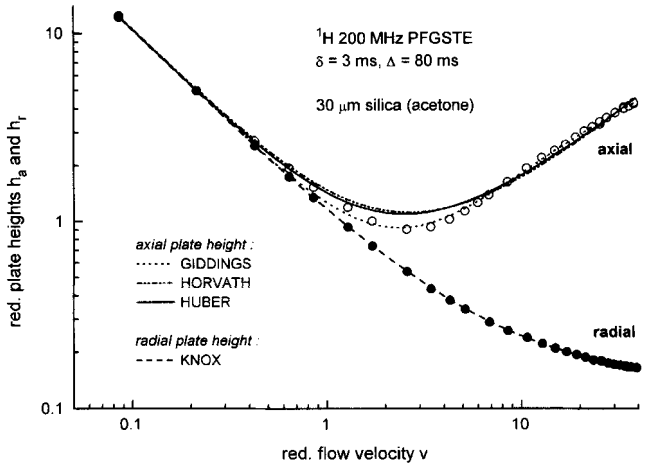

Figure 6. Axial reduced plate height vs. the reduced velocity.

Experimental data (symbols) compared with Eq. 4, with $x = 1$, 0.5, and 0.33 (lines). Column packed with 30-μm particles of silica from YMC. Solvent: acetone.

—Finally, for the data in Figure 4 (5-μm silica particles, methanol):

$$h_a = \frac{1.25}{\nu} + 0.642\nu^{0.33} + 0.088\nu \tag{19a}$$

$$h_r = \frac{1.23}{\nu} + 0.31. \tag{19b}$$

The confidence level of the fit of the reduced axial HETP was 0.996 and that of the fit of the reduced transverse HETP was 0.999 96. The coordinates of the minimum of the curve $h_a(\nu)$ are $h_{\min} = 1.53$ and $\nu_{opt} = 2.35$. These equations must be compared with those derived by Knox et al. (1976) (KLR), Eon (1978) (Eon), and Baumeister et al. (1995) (BKA). These authors obtained for the axial dispersion coefficient:

$$h_a(\text{KLR}) = \frac{1.4}{\nu} + 0.73\nu^{0.20}$$

$$h_a(\text{Eon}) = \frac{1.5}{\nu} + 0.64\nu^{0.21}$$

$$h_a(\text{BKA}) = \frac{0.994}{\nu} + 0.406\nu^{0.21} + 0.204\nu, \tag{20}$$

and for the radial (KLR, Eon) or the transverse (BKA) dispersion coefficient:

$$h_r(\text{KPR}) = \frac{1.4}{\nu} = 0.060$$

$$h_r(\text{Eon}) = \frac{1.5}{\nu} + 0.075$$

$$h_t(\text{BKA}) = \frac{0.994}{\nu} + 0.20. \tag{21}$$

We note that the values obtained in this work for the first coefficient, 2γ, in the case of large particles (Figure 2) in Eqs. 17a and 17b is in excellent agreement with the previous result of Baumeister et al. (1995), who used the same technique as ours, with a different instrument. They are, however, smaller than those obtained by authors using chromatographic methods. In the case of small particles, the value of this first coefficient is intermediate, 1.25 to 1.35, vs. 1 for previous NMR studies and 1.5 for chromatographic determinations. Note that the value obtained by Giddings and Robison for their exceptionally efficient column was 1.47, ruling out the possibility of a correlation between column efficiency and the value of γ.

The values of the second coefficient of the RHS of Eqs. 20 is much larger (by nearly 50%) in this work than in previous ones. The equations for the axial dispersion coefficient do not contain a $c\nu$ term in the cases of the measurements by Knox et al. (1976) and Eon (1978) because these authors used solid glass beads to pack their columns, while Baumeister et al. (1995) used porous particles for chromatography. Mass transfer through the particles used in this work seems somewhat faster than through those used previously (Lichrosorb). The radial dispersion coefficients were derived by Knox et al. (1976) and Eon (1978) by measuring the radial width of the elution band obtained with pointlike injection of the sample, using a syringe. An electrochemical detector with a microelectrode allowed the determination of the elution profiles at various distances from the column center. The precision of these determinations is certainly much lower than what can be achieved using the PFGNMR method.

Axial dispersion

The parameters of the PFGSTE NMR method used for the acquisition of the dispersion coefficients were slightly different in the three cases. The pulse width, δ, was 5 ms with the 5-μm silica particles and 3 ms with the 30-μm particles. The pulse period, Δ, was 80, 30 and 45 ms for the experimental results reported in Eqs. 17, 18 and 19, respectively. This gives a value of the mean dispersion distance, $[\langle r^2 \rangle]^{1/2}$, over which the data are averaged as 25.6, 12.8 and 13.1 μm, respectively, or approximately 90% of the average particle size with the 30-μm particle column and 2.5 of the particle diameter with the 5-μm particle column (using the Einstein relation and the values of the diffusion coefficients derived for the *pure* solvents; Table 1). Consequently, the dispersion distance is even lower in practice. This may explain some of the differences between the two different sets of data, especially regarding the value of the $b = 2\gamma$ coefficient in Eqs. 17 to 19. Note that, although the diffusion coefficient is lower inside the pore network of a porous particle than in the bulk mobile phase, the molecules have time in all these experiments to diffuse inside all the external space, around the particle, and inside most of the intraparticle space. We should anticipate that with the coarser particles, only the transchannel flow nonuniformities are sampled by the molecules. With the finer particles, both the transchannel and the short-range interchannel nonuniformities or at least part of the latter should be experienced.

The values obtained for the coefficient of the term accounting for molecular axial dispersion, $b = 2\gamma$, are in excellent agreement for all experiments performed on the same column. The values are 1.05 and 1.03 for the 30-μm particle column. For the 5-μm particle column, they are 1.35 and 1.32 for axial and transverse dispersion, respectively, with methanol, and 1.25 and 1.23, respectively, with acetonitrile/water. Assuming that the tortuosity coefficient, $\gamma = 1/T$ (T = conventional tortuosity) is close to the square root of the external porosity (Wong et al., 1984; Roberts and Schwartz, 1985), we obtain 0.27 and 0.41 as estimates of the external porosity of the two columns. The latter value is typical of analytical columns. It suggests a medium packing density, as allowed by the restriction placed by the limited mechanical strength of a PEEK tubing on the maximum flow rate that can be used during slurry packing. The former value seems unusually low compared to values obtained with random packing of this type of material under axial compression stress (Guiochon and Sarker, 1995; Sarker et al., 1995). The most probable explanation for this value is that the tortuosity model of dispersion in a packed bed is not valid when disper-

sion is measured over an average dispersion length of only 90% of the particle diameter. Dispersion has to take place over much longer distances for the tortuosity of the packed bed to be fully felt. The anomaly, however, is that value obtained is too low.

Figure 5 compares the experimental data (symbols) for axial dispersion and their best fit to the Knox equation (Eq. 17a). Two different values of n were used: the classic value used in chromatography, 0.33; the value used in early works (e.g., by Eon (1978)), 0.20. The second term of Eq. 9 seems to have no influence on the shape of the plot under the conditions that best fit our data. Indeed, the coefficient a is unusually small. This is in agreement with the extremely small value of the minimum plate height, 0.91, a value lower than most if not all those previously reported for porous particles in liquid chromatography. Obviously, the experimental conditions are different, there is no extracolumn band broadening under the experimental conditions of this work, and local values are measured. Nevertheless, this result is important because it tells how well the column is trying to work and how poorly we utilize its potential.

Figure 6 compares the experimental data obtained with the coarser particle column (symbols) and the curves corresponding to the best fit of these data to the Giddings (Eq. 4 with $x = 1$), Huber (Eq. 4 with $x = 0.5$), and Horvàth–Lin (Eq. 4 with $x = 0.33$) equations. Clearly, the Giddings equation gives by far the best fit. So, not surprisingly, our results agree with those of Magnico and Martin (1990). The differences between the experimental conditions used in their work and ours enhance the importance of this agreement. We used particles that are one to two orders of magnitude smaller than theirs. These particles are porous. Dispersion was measured *in situ*, without injection or any other external perturbation of the dynamics of the processes taking place in the column. Accordingly, the values obtained characterize the local axial and transverse HETP, not averages over the entire column volume as in the previous work.

The fit of the experimental data obtained with the coarser particles to the three equations 4, with $x = 1$ (Giddings, 1965), $x = 0.5$ (Huber, 1973), and $n = 0.33$ (Horvàth and Lin, 1976) gave residual standard deviations that are, respectively, 0.083, 0.382, and 0.575, confirming the conclusions of a visual examination of Figure 6. A considerable number of iterations was required in the last two cases, 172 and 38, respectively, and the best values obtained for γ and ω are physically meaningless. Stopping the nonlinear regression at the last set of physically meaningful values of these parameters lead to a standard deviation that is barely 10% higher than the previous ones. The best values of γ, λ, ω, and C obtained in the nonlinear regression of the experimental data using Eq. 4 (with $x = 1$) are $\gamma = 0.52$, $\lambda = 3.51$, $\omega = 35.3$, and $C = 0.015$ (Figure 2). These values should be compared with those obtained by Magnico and Martin (1990), $\gamma = 0.6$, $\lambda = 0.53$, $\omega = 10.3$, $C = 0$ (solid particles). The value of λ found by Magnico and Martin (1990) is the same as the one predicted by Giddings for the transchannel contribution. The value that we found for this parameter is seven times larger. It is consistent, however, with the assumption of a significant contribution of the transparticle effect that was inexistent in Magnico and Martin's experiment but is significant in ours. The value obtained for ω in this work is 3.5 times larger than that measured by Magnico and Martin (1990). This agrees with the much smaller contribution of the short-term interchannel effects to eddy diffusion that should be anticipated in our experimental conditions compared to theirs.

Transverse dispersion

The values obtained for the coefficient of the first term in Eqs. 17b, 18b, and 19b are practically equal to the values of the coefficient of the corresponding term in Eqs. 17a, 18a, and 19a. They are consistent with the indications given by theory in the derivation of Eq. 5 and with those of the stream-splitting model. These values were discussed in the previous section.

The numerical values of the coefficient D in Eq. 5 compare well with those reported in previous studies (Knox et al., 1976; Eon, 1978; Baumeister et al., 1995). Our values are 0.14 for the coarser particle column, 0.27 and 0.31 for the finer particle column, with acetonitrile/water and methanol, respectively. The value reported by Knox et al. (1976) was 0.060. The value obtained by Eon (1978) was 0.075. The value obtained by Baumeister et al. (1995) was 0.20 for 15-μm particles. In gas chromatography, Littlewood (1966) found an average value of $D = 0.20$, with results for individual columns ranging between 0.13 and 0.24, the larger values corresponding to the smaller particles (which is also the case for our results). Horne et al. (1966) concluded that values between 0.10 and 0.20 are the more probable. The results obtained regarding the axial dispersion coefficient have shown that the column packed with the coarser particles is the more efficient, that is, the better packed, whatever the reason it is so might be. We note also that Knox et al. (1976) and Eon (1978) were using large-size solid glass beads, about 60 and 76 μm in diameter, respectively. The center cores of their columns were extremely well packed as witnessed by the very low value of the reduced HETP they measured along the column axis (as opposed to the much higher values found close to the wall).

Axial dispersion measured: by NMR vs. by conventional chromatography

Figure 7 illustrates the considerable loss in potential performance that is incurred with the current procedures used in chromatography. The data in Figure 7b show what the column is trying to do, in terms of the local contribution to band broadening that takes place in the packing. The data in Figure 7a shows the overall effect, the actual amount of bank broadening produced. It is the corresponding bandwidth that controls the degree of separation achieved with the column in all practical applications of chromatography. The difference between the two sets of data stems from a combination of extra- and intracolumn contributions to band broadening. The former results from axial dispersion taking place in the sampling valve, the connecting tubes, the column ends, and the detector cell. This contribution is eliminated in PFGNMR. The latter contribution originates from the way the local contributions to band dispersion combine together. Because the bed is not homogeneous, the local axial velocity of the band depends on the location. The band profile become distorted. Although the band is locally very thin, all the parts of its profile do not reach the exit at the same time (Farkas et al.,

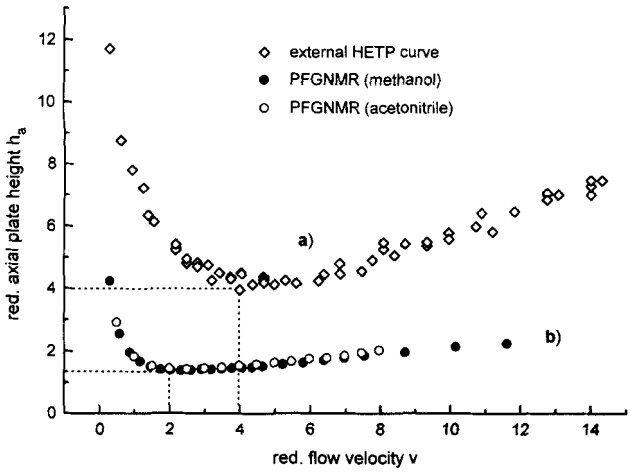

Figure 7. Reduced axial HETP derived: (a) conventional procedures of chromatography using the peaks recorded at the column outlet vs. analytical chromatograph; (b) axial dispersion coefficient determined by PFG NMR.

Experimental conditions, PEEK column packed with LiChrosorb RP18 5 μm. Solutes, (a) toluene, eluted with 80:20 acetonitrile/water as the mobile phase; (b) acetonitrile and methanol.

1994; Tallarek et al., 1995). This appears to cause most of the actual band spreading observed. Improving the degree of homogeneity of the packing obtained could allow a reduction of the column HETP by up to a factor of 3 (Figure 7).

Conclusion

Carefully conducted experiments, in which the contributions of the sources of extracolumn band broadening and the long-range interchannel effects are eliminated and the short-term channel effects are minimized, give values of the apparent axial dispersion coefficients whose flow velocity dependence supports the conclusions of the detailed analysis provided by Giddings (1965). This was the case in the experiments done by Magnico and Martin (1990). These authors used large-size glass beads that are easier to pack homogeneously than the small silica particles used in liquid chromatography. For a given value of the reduced HETP, the bands obtained are wider, thus contributing to minimizing the contributions of the sources of extracolumn band broadening. The same result was also accomplished by the design of their experimental setup. In our case, the principle of the method of measurement allows the acquisition of data under such conditions that only the short-range effects contribute to the result, while there are no sources of extracolumn band broadening. Our results confirm the validity of the Giddings equation in the range of Peclet numbers extending up to 40. Deviations may be expected at much higher values.

Further investigations involving the study of the influence of particle size and the mean dispersion distance, which increases as the square root of the pulse period, would allow the determination of the intraparticle dispersion and the study of the long-range interchannel effects (Giddings, 1965). This work could clarify a problem that has puzzled chromatographers for decades: Why is it that the actual efficiency of real columns is so poor compared to anticipations based on the predictions of the most reliable models?

Acknowledgments

This work has been supported in part by grant DE-FG0588ER13859 of the U.S. Department of Energy and by the cooperative agreement between the University of Tennessee and the Oak Ridge National Laboratory. We are grateful to J. C. Giddings (University of Utah) and M. Martin (Laboratoire de Physique et Mecanique des Milieux Heterogenes, ESPCI, Paris, France) for fruitful discussions, and to U. Trüdinger (YMC Europe) for the gift of the packing material. We acknowledge the continuous support of our computational effort by the University of Tennessee Computing Center. We thank the Alexander von Humboldt Stiftung (Bonn, Germany) for the Research Award received by one of the authors (G.G.) and the Deutsche Forschungsgemeinschaft for the support given to another of the authors (U.T.).

Literature Cited

Abragam, A., *Principles of Nuclear Magnetism*, Clarendon Press, Oxford (1961).

Arnold, F. H., H. W. Blanch, and C. R. Wilke, "Liquid Chromatography Plate Height Equations," *J. Chromatog.*, **330**, 159 (1985).

Baumeister, E., U. Klose, K. Albert, E. Bayer, and G. Guiochon, "Determination of the Apparent Radial and Axial Dispersion Coefficients in a Chromatographic Column by Pulsed Field Gradient Nuclear Magnetic Resonance," *J. Chromatog. A*, **694**, 321 (1995).

Baur, J. E., E. W. Kristensen, and R. M. Wightman, "Radial Dispersion from Commercial High-performance Liquid Chromatography Columns Investigated with Microvoltammetric Electrodes," *Anal. Chem.*, **60**, 2334 (1988).

Baur, J. E., and R. M. Wightman, "Microcylinder Electrodes as Sensitive Detectors for High-efficiency, High-speed Liquid Chromatography," *J. Chromatog.*, **482**, 65 (1989).

Bird, R. B., W. E. Stewart, and E. N. Lightfoot, *Transport Phenomena*, Wiley, New York (1960).

Callaghan, P. T., "Pulsed Field Gradient Nuclear Magnetic Resonance as a Probe of Liquid State Molecular Organization," *Aust. J. Phys.*, **37**, 359 (1984).

Callaghan, P. T., *Principles of Nuclear Magnetic Resonance Microscopy*, Oxford Univ. Press, Oxford (1991).

Callaghan, P. T., C. M. Trotter, and K. W. Jolley, "A Pulsed Field Gradient System for a Fourier Transform Spectrometer," *J. Magn. Reson.*, **37**, 247 (1980).

Cho, Z. H., J. P. Jones, and M. Singh, *Foundations of Medical Imaging*, Wiley, New York (1993).

Deelder, R. S., "Mobile-Phase Dispersion in Liquid Chromatography," *J. Chromatog.*, **47**, 307 (1970).

Ebach, E. A., and R. R. White, "Mixing of Fluids through Beds of Packed Solids," *AIChE J.*, **4**, 161 (1958).

Eon, C. H., "Comparison of Broadening Patterns in Regular and Radially Compressed Large-diameter Columns," *J. Chromatog.*, **149**, 29 (1978).

Farkas, T., J. Q. Chambers, and G. Guiochon, "Column Efficiency and Radial Homogeneity in Liquid Chromatography," *J. Chromatog.*, **679**, 231 (1994).

Farkas, T., M. J. Sepaniak, and G. Guiochon, "Column Radial Homogeneity in HPLC," *J. Chromatog.*, **740**, 169 (1996).

Gibbs, S. J., E. N. Lightfoot, and T. W. Root, "Protein Diffusion in Porous Gel Filtration Chromatography Media Studied by Pulsed Field Gradient NMR Spectroscopy," *J. Phys. Chem.*, **96**, 7458 (1992).

Giddings, J. C., "Evidence on the Nature of Eddy Diffusion in Gas Chromatography from Inert (Nonsorbing) Column Data," *Anal. Chem.*, **35**, 1338 (1963).

Giddings, J. C., *Dynamics of Chromatography*, Dekker, New York (1965).

Giddings, J. C., and R. A. Robison, "Failure of the Eddy Diffusion Concept of Gas Chromatography," *Anal. Chem.*, **34**, 885 (1962).

Godbille, E., and P. Devaux, "Use of an 18-mm I.D. Column for Analytical- and Preparative-Scale High-pressure Liquid Chromatography," *J. Chromatog.*, **222**, 317 (1976).
Guan, H., and G. Guiochon, "Reproducibility, Accuracy, and Correction of Isotherm Data Measured by Chromatography," *J. Chromatog. A*, **724**, 39 (1996).
Guiochon, G., and M. Sarker, "Consolidation of the Packing Material in Chromatographic Columns under Dynamic Axial Compression. I. Fundamental Study," *J. Chromatog.*, **704**, 247 (1995).
Guiochon, G., S. G. Shirazi, and A. M. Katti, *Fundamentals of Nonlinear and Preparative Chromatography*, Academic Press, Boston, (1994).
Gunn, D. J., "Theory of Axial and Radial Dispersion in Packed Beds," *Trans. Inst. Chem. Eng.*, **47**, T351 (1969).
Gunn, D. J., "Mixing in Packed and Fluidised Beds," *Chem. Eng.*, **46**, CE153 (1968).
Hahn, E. L., "Spin Echoes," *Phys. Rev.*, **80**, 580 (1950).
Halasz, I., and E. Heine, "Separation of Low-Boiling Hydrocarbons by Gas Chromatography using Packed Capillary Columns," *Nature*, **194**, 971 (1962).
Hiby, J. W., *Interaction between Fluids and Particles*, P. A. Rottenburg, ed., Institution of Chemical Engineers, London, p. 312 (1962).
Horne, D. S., J. H. Knox, and L. McLaren, "A Comparison of Mobile Phase Peak Dispersion in Gas and Liquid Chromatography," *Sep. Sci. Technol.*, **1**, 531 (1966).
Horvàth, C., and H.-J. Lin, "Movement and Band Spreading of Unsorbed Solutes in Liquid Chromatography," *J. Chromatog.*, **126**, 401 (1976).
Horvàth, C., and H.-J. Lin, "Band Spreading in Liquid Chromatography. General Plate Height Equation and a Method for the Evaluation of the Individual Plate Height Contributions," *J. Chromatog.*, **149**, 43 (1978).
Huber, J. F. K., "Stofftransport and Stoffverteilung bei Chromatographischen Prozessen," *Ber. Bunsenges. Phys. Chem.*, **77**, 179 (1973).
Kärger, J., H. Pfeifer, and W. Heink, "Principles and Applications of Self-diffusion Measurements by Nuclear Magnetic Resonance," *Adv. Magn. Reson.*, **12**, 1 (1988).
Kärger, J., and D. M. Ruthven, *Diffusion in Zeolites and Other Microporous Solids*, Wiley, New York (1992).
Katz, E., K. L. Ogan, and R. P. W. Scott, "Peak Dispersion and Mobile Phase Velocity in Liquid Chromatography: The Pertinent Relationship for Porous Silica," *J. Chromatog.*, **270**, 51 (1983).
Kennedy, J. G., and J. H. Knox, "The Performance of Packings in High Performance Liquid Chromatography. I. Porous and Surface Layered Supports," *J. Chromatog. Sci.*, **10**, 549 (1972).
Knox, J. H., and M. Saleem, "Kinetic Condition for Optimum Speed and Resolution in Column Chromatography," *J. Chromatog. Sci.*, **7**, 614 (1969).
Knox, J. H., G. R. Laird, and P. A. Raven, "Interaction of Radial and Axial Dispersion in Liquid Chromatography in Relation to the 'Infinite Diameter Effect'," *J. Chromatog.*, **122**, 129 (1976).
Knox, J. H., "Practical Aspects of LC Theory," *J. Chromatog. Sci.*, **15**, 352 (1977).
Komoroski, R. A., "Nonmedical Applications of NMR Imaging," *Anal. Chem.*, **65**, 1068A (1993).
Little, J. N., R. L. Cotter, J. A. Prendergast, and P. D. McDonald, "Preparative Liquid Chromatography using Radially Compressed Columns," *J. Chromatog.*, **126**, 439 (1976).
Littlewood, A. B., "Relative Contributions of Molecular Diffusion and Anastomosis in Gas Chromatographic Columns," *Anal. Chem.*, **38**, 2 (1966).
Magnico, P., and M. Martin, "Dispersion in the Interstitial Space of Packed Columns," *J. Chromatog.*, **517**, 31 (1990).
Mills, R., "Self-diffusion in Normal and Heavy Water in the Range 1–45°," *J. Phys. Chem.*, **77**, 685 (1973).
Pfeffer, R., and J. Happel, *AIChE J.*, **10**, 605 (1964).
Poole, C. F., and S. K. Poole, *Chromatography Today*, 2nd ed., sec. 4.3, Elsevier, Amsterdam, The Netherlands (1993).
Roberts, J. N., and L. M. Schwartz, "Grain Consolidation and Electrical Conductivity in Porous Media," *Phys. Rev. B*, **31**, 5990 (1985).
Saffman, P. G., "A Theory of Dispersion in a Porous Medium," *J. Fluid Mech.*, **6**, 321 (1959).
Saffman, P. G., "Dispersion Due to Molecular Diffusion and Macroscopic Mixing in Flow Through a Network of Capillaries," *J. Fluid Mech.*, **7**, 194 (1960).
Sarker, M., A. M. Katti, and G. Guiochon, "Consolidation of the Packing Material in Chromatographic Columns under Dynamic Axial Compression: II. Consolidation and Breakage of Several Packing Materials," *J. Chromatog.*, **719**, 275 (1996).
Slichter, C. P., *Principles of Magnetic Resonance*, Harper & Row, New York (1963).
Stanley, B., M. Sarker, and G. Guiochon, "Consolidation of the Packing Material in Chromatographic Columns under Dynamic Axial Compression: IV. Mechanical Properties of Some Packing Materials," *J. Chromatog.*, **741**, 175 (1996).
Stejskal, E. O., "Use of Spin Echoes in a Pulsed Magnetic Field Gradient to Study Anisotropic, Restricted Diffusion and Flow," *J. Chem. Phys.*, **43**, 3597 (1965).
Stejskal, E. O., and J. E. Tanner, "Spin Diffusion Measurements: Spin Echoes in the Presence of a Time Dependent Field Gradient," *J. Chem. Phys.*, **42**, 288 (1965).
Sternberg, J. C., and R. E. Poulson, "Particle-to-Column Diameter Ratio Effect on Band Spreading," *Anal. Chem.*, **36**, 1492 (1964).
Stilbs, P., "Fourier Transform Pulsed-Gradient Spin-Echo Studies of Molecular Diffusion," *Prog. NMR Spectrosc.*, **19**, 1 (1987).
Tallarek, U., E. Baumeister, K. Albert, E. Bayer, and G. Guiochon, "NMR Imaging of the Chromatographic Process. Migration and Separation of Bands of Gadolinium Chelates," *J. Chromatog.*, **696**, 1 (1995).
Tanner, J. E., "Use of the Stimulated Echo in NMR Diffusion Studies," *J. Chem. Phys.*, **52**, 2523 (1970).
Tanner, J. E., and E. O. Stejskal, "Restricted Self-diffusion of Protons in Colloidal Systems by the Pulsed-Gradient, Spin-Echo Method," *J. Chem. Phys.*, **49**, 1768 (1968).
Train, D., "Transmission of Forces through a Powder Mass during the Process of Pelleting," *Trans. Inst. Chem. Eng.*, **35**, 258 (1957).
Unger, K. K., W. Messer, and K. F. Krebs, "Comparative Study of the Performance of Spherical and Angular Silica and Alumina Supports in the 1–10-μm Size Range," *J. Chromatog.*, **149**, 1 (1978).
Van Deemter, J. J., F. J. Zuiderweg, and A. Klinkenberg, "Longitudinal Diffusion and Resistance to Mass Transfer as Causes of Nonideality in Chromatography," *Chem. Eng. Sci.*, **5**, 271 (1956).
Wehrli, F. W., D. Shaw, and J. B. Kneeland, eds., *Biomedical Magnetic Resonance Imaging*,, VCH, New York (1988).
Wong, P.-Z., J. Koplik, and J. P. Tomanic, "Conductivity and Permeability of Rocks," *Phys. Rev. B*, **30**, 6606 (1984).
Yun, T., and G. Guiochon, "The Modeling of Radial Heterogeneity in Chromatographic Columns. Cylindrical Column and Ideal Model, *J. Chromatog.*, **672**, 1 (1994).

Manuscript received Jan. 16, 1996, and revision received Apr. 15, 1996.